For. Sci. 60(x):000–000
http://dx.doi.org/10.5849/forsci.13–025

forest ecology

Landscape-Scale Influence of Topography on Organic Layer Accumulation in Paludified Boreal Forests

Ahmed Laamrani, Osvaldo Valeria, Nicole Fenton, and Yves Bergeron

The aim of this study was to quantitatively investigate the relationship between topographic variables and organic layer thickness (OLT) and to use these relationships for mapping OLT distributions at the landscape scale within the paludified boreal forests of eastern Canada. Topography was quantified by a set of predictor variables (slope, elevation, aspect, mean curvature, plan curvature, and profile curvature) that were extracted from a LiDAR-derived digital terrain model (DTM) with four resolutions (1, 5, 10, and 20 m). OLT was collected from field measurement ($n = 1,600$) across the landscape and varied from 5 to 150 cm. Weak correlations between OLT and individual topographic variables were obtained at the landscape scale. Stratification by aspect did not significantly improve these correlations. Consequently, regression tree analysis divided the data into six different landscape units, based on slope, aspect, and mean curvature. The resulting landscape units delimited the major patterns of OLT and elucidated three spatial relationships between OLT and topographic variables: greater OLTs (mean = 62 cm) were confined to gentle slopes ($\leq$1.8%), whereas lower OLTs (mean = 27 cm) were found in steeper slopes (slope $>$3.2%); OLTs were deeper on south- and west-facing than on north- and east-facing slopes; and the most accurate results were obtained by the LiDAR-derived DTM at 10- and 20-m resolutions. A thematic productive map of the distribution of the resulting six landscape units showed good matching (71%) with both vulnerable and promising areas for forest management. This study confirmed the fact that topographic variables influence OLT at the landscape scale, which had been previously reported at the plot scale within the Clay Belt.

Keywords: paludification, topography, Clay belt, regression tree, LIDAR-derived digital terrain model

Boreal northern black spruce forests are characterized by the development of thick organic layers in regions prone to paludification such as the interior of Alaska, the Canadian Hudson Bay-James Bay lowlands, and the western Siberian plain. Paludification is a natural process in which organic material accumulates on the forest floor over time and is generally thought to be caused by increasing soil moisture (Crawford et al. 2003, Vygodskaya et al. 2007). This process creates wetter conditions that lead over time to a reduction in soil temperature, decomposition rates, microbial activity, and nutrient availability (Lavoie et al. 2005). This promotes the growth of sphagnum mosses (Fenton et al. 2005, Fenton and Bergeron 2007) and the conversion of potentially forested areas to large bog landscapes, largely resistant to forest establishment and growth (Crawford et al. 2003), consequently, leading to a marked decrease in forest productivity (Simard et al. 2007, 2009). In addition to these factors, time since last fire and topography play important roles in the occurrence of paludification in these regions. Although the effect of topography on organic layer thickness (OLT) has been well studied at the plot scale, there is no research, to our knowledge, documenting the effect of topography at the landscape scale.

In the Clay Belt, a region of the Hudson Bay-James Bay lowlands of boreal eastern Canada, OLT usually displays high spatial variability both at the landscape and plot scale. This variability in OLT within Clay Belt black spruce forests is largely influenced by time since last fire and topography. Moreover, an understanding of the

Manuscript received February 18, 2013; accepted July 23, 2013; published online September 19, 2013.

Affiliations: *Ahmed Laamrani (ahmed.laamrani@uqat.ca), Institut de recherche sur les forêts, Université du Québec en Abitibi-Témiscamingue, Rouyn-Noranda, QC, Canada. Osvaldo Valeria (osvaldo.valeria@uqat.ca), Institut de recherche sur les forêts, Université du Québec en Abitibi-Témiscamingue. Nicole Fenton (nicole.fenton@uqat.ca), Institut de recherche sur les forêts, Université du Québec en Abitibi-Témiscamingue. Yves Bergeron (yves.bergeron@uqat.ca), Institut de recherche sur les forêts, Université du Québec en Abitibi-Témiscamingue.*

Acknowledgments: *This research was supported by the Natural Sciences and Engineering Research Council of Canada (NSERC), Fonds Québécois de la Recherche sur la Nature et les Technologies (FQRNT), the Université du Québec en Abitibi-Témiscamingue (UQAT), NSERC-UQAT-Université du Québec à Montréal (UQAM) Chair in Sustainable Forest Management, the Regional Conference of Elected representatives of James Bay, Centre d'Étude de la Forêt-Centre of Forest Research (CEF-CFR) and Tembec, Inc. We are grateful to Dr. Benoît St-Onge from the UQAM for his assistance with the processing of raw LiDAR data and to Dr. W.F.J. Parsons from the CEF-CFR, who revised the English and helped improve the quality of the manuscript. We thank the associate editor and anonymous reviewers for their helpful comments throughout the review process.*

causes of this variability is important for accurately predicting the locations of highly paludified areas as well as their impacts on forest management. Consequently, there is an increasing practical demand for maps that contain information concerning variation in OLT and topography in paludified areas. The end users of this information are involved mainly in forest management (i.e., forest planning and productivity assessment).

Within paludified forests, there have been few studies that describe or analyze topographic factors that influence the spatial distribution and accumulation of organic layers at larger scales (i.e., Emili et al. 2006, Seibert et al. 2007). Other studies have been conducted at larger scales to characterize the influence of topography on soil properties; however, these studies have been largely restricted to well-drained hardwood in the south of the boreal forest (i.e., Martin and Timmer 2006, Johnson et al. 2009). Previous studies that have tried to relate OLT to topography in the Clay Belt region have been limited to either the plot scale or to only slope estimates as the controlling variable (Giroux et al. 2001, Fenton et al. 2005, Lavoie et al. 2005, Lecomte et al. 2005, Simard et al. 2007, 2009). As yet, no research has tested whether the plot-scale relationship between slope and OLT can be observed at larger scales (i.e., landscape scale) or whether other topographic variables could influence OLT individually or in combination with slope. Until recently, the availability of accurate topographic information regarding the organic layer at larger scales (landscape or regional) was a limiting factor for both land management and modeling of spatial OLT variability. Recent advances in remote sensing now permit the generation of appropriate data for determining these relationships. Consequently, there is much interest in relating different OLT information to high-resolution topographic data. These data, in turn, can be used to generate topographic variables such as slope, aspect, elevation, or curvature. In this context, high-resolution airborne laser scanning (also known as LiDAR [light detection and ranging]) is becoming one of the most effective and reliable remote-sensing technologies for assessing topography at both the plot and landscape scales in boreal forested environments (i.e., Hodgson et al. 2003, 2005, Hyde et al. 2005, Webster et al. 2011, Work et al. 2011, Southee et al. 2012). The objective of this study was to quantitatively investigate the relationship between topographic variables and OLT and to use these relationships for mapping OLT distributions at the landscape scale within the black spruce forests of the Clay Belt. To do so, we correlated field OLT measurements (response variable) obtained by manual probing with topographic variables (predictor variables) derived from LiDAR digital terrain models (DTMs).

Materials and Methods

Study Area

The study sites were located within an area of approximately 720 ha of boreal forest in the southwestern James Bay Lowlands physiographic region of Quebec and, more precisely, in the Clay Belt region that spans 125,000 km^2, mainly above 49°N across the Ontario-Quebec border (Figure 1A). This study is part of a larger project that deals with the effects of environmental variables and forest harvesting on paludification. The dominant landforms in the area are gently sloping plains, which were generated by extensive and thick glaciolacustrine clay deposits left behind by the proglacial Lake Ojibway (Veillette 1994). Bedrock outcrops and gentle hills are also found in the area. Elevation ranges between 289 and 315 m, with an average of 304 m above sea level. Within the study area, ground surface slope ranged from 0.1 to 14.9%; about 45% of the area had a slope ≤2%. Many drainage courses run locally in a southwestern direction through the study area to produce a relatively complex topographic pattern in this hilly landscape relief (Figure 1B).

Black spruce (*Picea mariana* [Mill.] BSP) and jack pine (*Pinus banksiana* Lamb.) dominate stands in the study area, constituting 79 and 16% of the canopy, respectively. These species are followed by trembling aspen (*Populus tremuloides* Michx), which occupies about 4% of the study area. The remaining 1% of the area is covered by tamarack or eastern larch (*Larix laricina* [Du Roi] K. Koch), balsam fir (*Abies balsamea* [L.] Miller), and paper birch (*Betula papyrifera* Marshall). The forest floor is composed of *Sphagnum* spp., feather mosses (principally *Pleurozium schreberi* [Brid.] Mitten), and shrubs, (mainly dwarf ericaceous species), with variable coverage across the landscape. The mean annual temperature is −0.7° C, and the mean annual precipitation is 906 mm (Environment Canada 2011; Matagami weather station, approximately 60 km northeast of the study area).

Sampling Design and Field Data Collection

The study goals were addressed by establishing transects over representative forest stands at the landscape scale. We used provincial Forest Inventory Maps from the Quebec Ministry of Natural Resources (MRNQ) within a geographic information system (GIS) and information collected during field visits to select stands representing a broad range of OLT, slope inclinations, and stand productivities. Such attributes were obtained from the interpretation of data available from the Forest Inventory Maps of the MRNQ (i.e., cover density classes, age classes, species, height classes, and slope classes).

For the purposes of providing a spatially continuous cross-sectional profile of OLT at the landscape scale, field data were acquired along and between continuous transects. Thirteen transects, totaling 15 km in length, were established across four different sectors, running from northeast to southwest (sectors 2 and 3) and northwest to southeast (sectors 1 and 4) (Figure 1B). Within each sector, a minimum of 20 m was maintained between transects, and OLT was measured manually using a standard auger at intervals of 10 m along each transect. At each sampling point, the auger bored through the organic layer until the mineral soil was encountered. The auger was then removed, and the marked depth to mineral soil was accurately measured (OLT ranging from 5 to 125 cm) (Figure 2). The thickness of the organic material was taken as the distance between the organic layer surface and the mineral soil interface. In nearly all cases, the transition between the organic layer and mineral soil was clearly marked by an obvious change in color and texture (Figure 2). When the full length of the auger (=125 cm) was inserted into the organic layer without contacting the mineral soil, the corresponding point was marked as deeper than 125 cm. These sites were excluded because it was technically impossible to measure depths greater than 125 cm while measuring so many points. There are only 17 sites (about 1% of the entire data) that were excluded from the analysis, which should not affect the result. An additional 85 circular plots of 400 m^2 were randomly distributed between transects over the study area and sampled for forest canopy measurements, soil samples (not included in this article), and organic layer information. A 30 × 30-cm pit was dug in each of the 85 plots and depth to mineral soil (total OLT, ranging from 7 to 150 cm) was recorded, together with an accurate measurement of the thickness of each individual soil organic horizon (cm). For the entire data set (n = 1,600; sampling points along transects and plots), the nature of

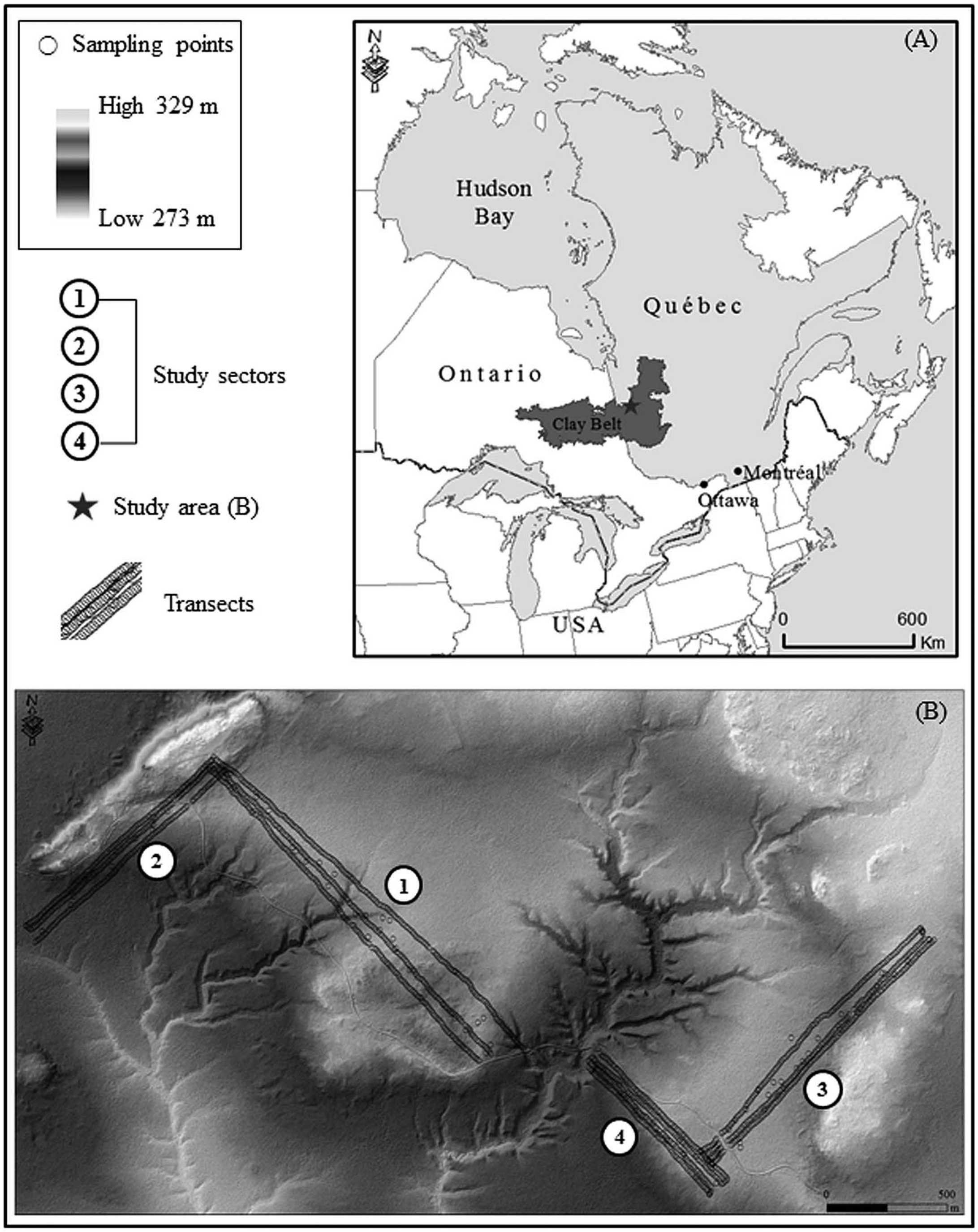

Figure 1. Study area located in the Clay Belt region (A) with a DTM derived from LiDAR data (B) and sampling point locations along 13 transects that were established across four sectors (1, 2, 3, and 4).

the underlying mineral deposits was recorded in the field as clay, till, or bedrock; however, their effects, together with those of time-since-last fire, on OLT were not examined in this study, because they will be dealt with in a future study.

LiDAR Processing and Topographic Variable Measurements

LiDAR data were collected over the study area in late May 2010 using a Multipulse Leica ALS50 phase II airborne laser scanner. LiDAR acquisition was conducted with an average sampling of 2.8 points/m^2 and an absolute vertical accuracy of 0.065 m (root mean square error). All collected LiDAR data were preprocessed by separating canopy pulse returns from ground pulse returns. Inverse distance weighting was used as the grid interpolating model and for predicting *z* values within the study area. The latter data were used to produce a DTM with a basic cell resolution (cell size) of 0.5 m using ArcGIS 10.0 (Environmental Systems Research Institute [ESRI] 2011). Spatial Analyst tools (ArcGIS) were used to generate different DTMs of the selected topographic variables at four cell resolutions (1, 5, 10, and 20 m). A detailed description of each selected topographic variable (elevation, slope, aspect, mean curvature, plan curvature, and profile curvature) is provided in Table 1. The DTM cell corresponding to each field sampling point was determined and the values of its topographic variables were calculated at the four cell resolutions. These data were used for two

Figure 2. Photographs from the study area. At each sampling point, the auger was bored through the organic layer until the mineral soil was encountered (A and B) and then the depth to mineral soil (represents the OLT) was clearly identified (pointer finger on C) and measured (distance between flag mark and pointer finger on D).

Table 1. Topographic variables measured from LiDAR-derived DTMs of the study area.

Topographic variables	Description
Slope	Gradient or rate of maximum change in *z* value from each cell of a raster surface (%).
Elevation	Refers to how high above sea level a particular location in the study area is; also known as *z* value (m).
Aspect	Direction of the maximum rate of change in the *z* value from each cell to its neighbors. The value of each cell in an aspect data set (0° up to 360°) indicates the direction the cell's slope faces (N, NE, E, SE, S, SW, or NW). Each of these directions represents an interval of 22.5°.
Mean curvature†	Represents the roughness of the terrain and corresponds to the second derivative of the surface or the slope of the slope. A positive curvature indicates that the surface is upwardly convex at that cell, whereas a negative curvature indicates the surface is upwardly concave at that cell. Profile and plan are two output curvature types.
Plan curvature	Perpendicular to the direction of the maximum slope. Sidewardly convex surfaces have a positive value, sidewardly concave surfaces have a negative plan, and linear areas have a value of zero. Profile curvature relates to the convergence and divergence of flow across a surface.
Profile curvature	Parallel to the direction of the maximum slope. Upwardly convex surfaces have a negative value, upwardly convex surfaces have a positive plan, and flat areas have a value of zero. Profile curvature affects the acceleration or deceleration of flow across the surface.

The reasonably expected values of curvature rasters (curvature, plan, and profile) for a hilly area (moderate relief) can vary from −0.5 to 0.5, whereas for steep, rugged mountains (extreme relief), the values can vary between −4 and 4 (ESRI 2011).

purposes: to determine how the extracted values of topographic variables are sensitive to DTM resolutions and to evaluate the correlations between the OLT and individual topographic variables.

Statistical Analysis

Preliminary statistical analysis was done using backward stepwise linear regression to investigate which topographic variables significantly influence OLT at the landscape scale. All topographic variables that were used in the stepwise regression analysis were tested for multicollinearity and their coefficients of variation (CVs), which were calculated as their SDs divided by the respective means, were used to evaluate the distribution of the data and the interactions between different topographic variables and OLT. Two nonparametric methods, Spearman's rank correlation and regression tree analysis, were also used. Because many of the topographic variables were highly intercorrelated (Pearson's $r \geq 0.7$) and had highly skewed distributions, we used Spearman's rank correlation (r_s) instead the usual parametric product-moment correlation coefficient (r). Spearman's coefficient has been used in similar studies with larger data sets that are characterized by a high degree of heterogeneity (e.g., Seibert et al. 2007, $n = 1{,}300–4{,}000$ points). The high CVs (>0.56) for OLT also suggested that the data had a strongly skewed distribution. For these reasons, no attempt was made to explore the relationships between OLT and topographic variables using multiple regression or linear mixed-effects models.

A common way of spatially segmenting the landscape is to divide it into internally homogeneous and mutually contrasting units (Mulder et al. 2011). Landscape segmentation involves grouping similar topographic variables into distinct spatial units, which can then be used as treatments for spatial analysis (Pennock and Corre 2001). Therefore, we used regression tree analysis as an automated landscape segmentation method to identify spatial units that could empirically model the complex interactions among topographic variables in controlling OLT distribution. The regression tree approach was well suited to the analysis of our data sets for several reasons: (1) its potential to successfully predict soil organic matter distribution and to analyze ecological data has been demonstrated (i.e., De'Ath and Fabricius 2000, Johnson et al. 2009, Häring et al. 2012); (2) it is capable of handling both categorical and quantitative data (Johnson et al. 2009); (3) it allows complex interactions among predictor variables with no assumptions of linearity (Rothwell et al. 2008); (4) the regression tree method repeatedly splits the response data (in our case, OLT) into more homogeneous groups, based on the predictor variables and predictor values (or identifiers, if categorical, i.e., aspect variable), which results in a tree diagram that is easy to read and interpret (Johnson et al. 2009); and (5) recursive partitioning of the data set into more homogeneous groups allows the identification of potential relationships between the response variable and the environmental predictors, while also identifying interactions among these latter independent variables (Rothwell et al. 2008). In each resulting spatial unit, rules defining how the data were to be partitioned were selected based on a significance test of independence between covariates and the response variable, and a split was established when the P value was smaller than $\alpha = 0.05$ (Hothorn et al. 2006). In this study, the resulting spatial units were named "landscape units" that refer to relatively homogeneous areas in term of OLT distribution. All statistical analyses were performed in R (R Development Core Team 2011). Regression trees were implemented using the ctree function in the party package (Hothorn et al. 2006).

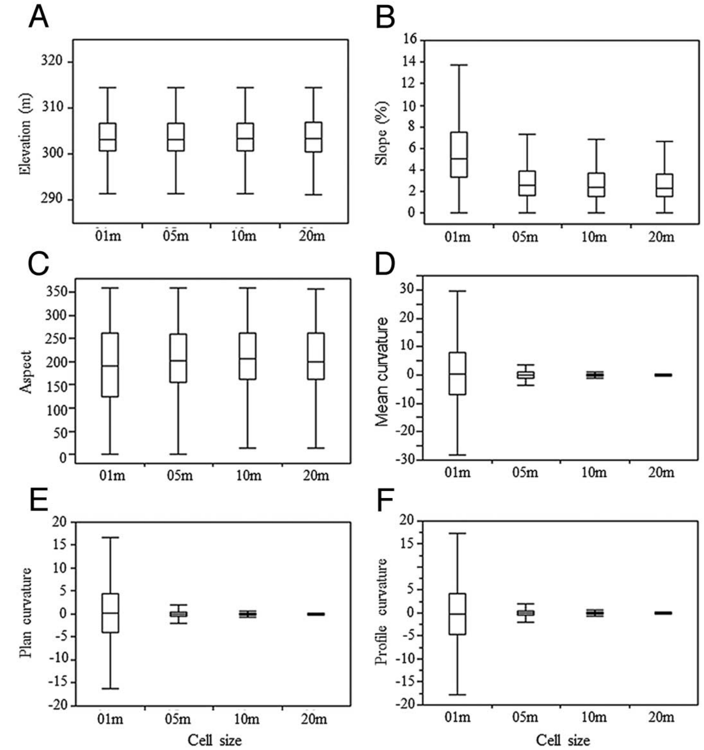

Figure 3. Box plots of topographic variables for four DTM resolutions. (A) Elevation. (B) Slope. (C) Aspect. (D) Mean curvature. (E) Plan curvature. (F) Profile curvature. The lower and upper edges of the box represent the 25th and 75th percentiles, and the median is represented by the band in the middle of the box. Whiskers represent the lower and upper extremes (lowest and highest values, respectively).

Results

Effect of Different LiDAR-Derived DTM Resolutions on the Values of Topographic Variables

Figure 3 shows that both elevation and aspect are invariant with changes in resolution, whereas variation strongly decreased as spatial resolution decreased for the mean curvature, plan curvature, and profile curvature. Median and range estimates of elevation did not indicate significant bias (Figure 3A), whereas those of slope decreased markedly with decreasing resolution (Figure 3B). Aspect did not show any obvious trends across the different resolutions (Figure 3C). The range of values of all curvature variables (curvature, plan, and profile) decreased clearly with decreasing resolution, whereas the medians did not vary with changes in resolution (Figure 3D−F).

Correlations Between OLT and Topographic Variables Based on Different DTM Resolutions

Extracted values of topographic variables at each sampling point were used to graphically illustrate and evaluate the effect of resolution on OLT (Figure 4; Table 2). Even though Spearman's rank correlations were considered weak ($r_s \leq 0.56$) (Table 2), most were statistically significant and provided some insight into which factors influenced the spatial distribution and accumulation of the organic layer at the landscape scale. Of the topographic variables examined, slope had the strongest correlation with OLT across the 5- to 20-m DTM resolutions. Across all DTMs resolutions, slope was consistently and negatively related to OLT ($P < 0.001$). Figure 4A illustrates the tendency of OLT to generally decrease with increasing slope over the landscape.

Elevation and OLT were significantly positively correlated ($r_s = 0.12$, $P < 0.001$) at all resolutions. However, the correlation is weak ($r_s = 0.12$) as illustrated by the marked scatter of the data (Figure 4B), and no clear trend could be seen when the whole data set was used ($n = 1,600$).

The reasonably expected values of plan and profile curvatures variables (extracted from LiDAR-derived DTM) for our study area (moderate relief) should vary from −0.5 to 0.5 (ESRI 2011). However, 72 to 97% of plan and profile curvatures values at 1- and 5-m resolutions were outside this expected range and consequently were excluded from the analysis. At the 10- and 20-m resolutions, the correlation between OLT and all curvature variables indicated that OLT tended to decrease with convexity. This result is in accord with landscape observations for which thinner organic layers are habitually associated with areas having convex slopes. At the 10- and 20-m resolutions, coefficients of correlations were significantly higher for convex curvatures (mean, plan, and profile) than those for the concave curvatures. All correlations between concave curvatures (mean, plan, and profile) and OLT were very small and not significant at the 1- and 10-m resolutions (Table 2).

Because aspect was not measured on a linear scale (circularly disturbed), it was excluded from the correlation analysis (Table 2). To determine whether correlations between OLT and other topographic variables improved with aspect stratification, correlations

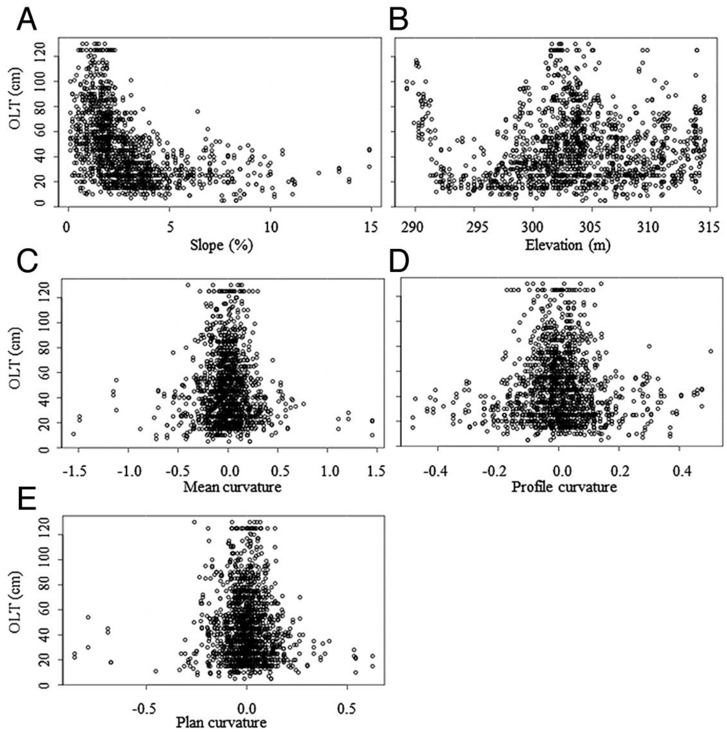

Figure 4. Relationships Between OLT and topographic variables at 20-m DTM resolution (n = 1,600). (A) Slope. (B) Elevation. (C) Mean curvature. (D) Profile curvature. (E) Plan curvature.

Table 2. Spearman rank correlations Between OLT and topographic variables at different DTM resolutions.

Topographic variables	r_s at DTM resolution of 01 m	05 m	10 m	20 m
Slope	−0.13*	−0.46*	−0.53*	−0.56*
Elevation	0.12*	0.12*	0.12*	0.12*
Mean curvature [Convex]	−0.01	0.01	−0.15*	−0.25*
Mean curvature [Concave]	−0.00	−0.08†	0.06	0.14*
Plan curvature [Convex]	−0.01	−0.02	−0.12*	−0.22*
Plan curvature [Concave]	−0.06	−0.09‡	0	0.08†
Profile curvature [Convex]	−0.00	0.01	0.15*	0.27*
Profile curvature [Concave]	−0.02	0.08†	−0.07	−0.16*

n = 1,600.
* $P < 0.001$.
† $P < 0.01$.
‡ $P < 0.05$.

Table 3. OLT data for major aspect classes for the study area.

Variable	n	OLT Mean (cm)	SD (cm)	CV
North	57	45	19	0.42
Northeast	32	43	15	0.35
East	82	35	16	0.46
Southeast	224	39	25	0.64
South	459	43	28	0.65
Southwest	231	53	28	0.53
West	386	48	22	0.46
Northwest	129	44	19	0.43
All data	1600	45	25	0.56

n represents number of sampling points.

between OLT and topographic variables were calculated for main aspect classes, which are summarized in Tables 3 and 4 (20-m resolution data only). From Table 3, we can deduce that 81% of sampling points had an aspect ranging from southeast (southeast [SE], south [S], or southwest [SW]) to west (W), whereas only 19% had a northern (northwest [NW], north [N], or northeast [NE]) or eastern (E) exposure. Average OLT in areas with southern and western aspects (SE + S + SW + W) was higher than that in areas with northern or eastern aspects (NW + N + NE + E). In addition, CVs for OLT were relatively high (≥0.35), suggesting that aspect stratification did not notably reduce the variability within most of the aspect classes and the existence of interactions between different landscape topographic variables and OLT.

Results of Spearman's rank correlations between OLT and individual topographic variables for each major aspect class, as well as their improvement or diminution with regard to all the data, are shown in Table 4. Δr_s values were calculated as the absolute r_s for the aspect class minus the absolute r_s of all the data (n = 1,600) listed in Table 3. After aspect stratification, most coefficients were still very small or not significant, even though some strong relationships existed between the S, SE, W, and N classes and OLT, especially for 10- and 20-m resolutions.

The correlation between slope and OLT for the S aspect class was significantly improved with respect to the collective data set ($r_s = -0.70$, $P < 0.001$, and $\Delta r_s = 0.14$). This relation, in which OLT increased as slope decreased in the S aspect, is illustrated in Figure 5A. To test the significance of Δr_s, we performed an omnibus test of homogeneity among the eight aspect classes ($k = 8$) in terms of their Spearman's rank correlations, which takes the form of a χ^2-distributed test. For example, at the 20-m resolution, estimates of slope correlations with OLT indicated very strong differences among the eight aspect classes in Table 4 (overall $\chi^2 = 92.85$, $df = 7$, $P < 0.001$).

Table 4. Spearman's rank correlation between OLT and topographic variables for each major aspect class.

Cell size and variable	N r_s	N Δr_s	NE r_s	NE Δr_s	E r_s	E Δr_s	NW r_s	NW Δr_s	SE r_s	SE Δr_s	S r_s	S Δr_s	SW r_s	SW Δr_s	W r_s	W Δr_s
1 m																
Slope	−0.14	0.01	−0.07	−0.06	−0.13	0.00	0.01	−0.12	−0.16†	0.03	−0.27[a,*]	0.14	−0.10	−0.03	−0.08	−0.05
Elevation	0.05	−0.07	0.16	0.04	−0.02	−0.10	0.25[a,*]	0.13	0.00	−0.12	0.04	−0.08	0.22*	0.10	0.21*	0.09
Curvature [Convex]	−0.21	0.20	−0.17	0.16	−0.12	0.11	0.15	0.14	−0.04	0.03	0.06	0.05	0.12	0.11	−0.04	0.03
Curvature [Concave]	0.10	0.10	−0.07	0.07	0.03	0.03	0.10	0.10	0.04	0.04	−0.06	0.06	0.02	0.02	−0.02	0.02
Plan [Convex]	−0.12	0.11	−0.16	0.15	−0.12	0.11	0.06	0.05	0.02	0.01	0.00	−0.01	0.22[a,†]	0.21	−0.04	0.03
Plan [Concave]	−0.09	0.03	−0.04	−0.02	−0.01	−0.05	0.09	0.03	−0.03	−0.03	−0.14	0.08	−0.04	−0.02	−0.05	−0.01
Profile [Convex]	0.22[b,†]	0.22[b]	0.03	0.03	0.23[b,†]	0.23	−0.03	0.03	−0.02	0.02	−0.08	0.08	−0.03	0.03	−0.12	0.12
Profile [Concave]	0.08	0.06	0.00	−0.02	0.11	0.09	0.00	−0.02	−0.05	0.03	−0.10	0.08	−0.10	0.08	0.04	0.02
5 m																
Slope	−0.27*	−0.19	−0.40*	−0.06	−0.24†	−0.22	−0.44*	−0.02	−0.51*	0.05	−0.53[a,*]	0.07	−0.41*	−0.05	−0.40*	−0.06
Elevation	0.20	0.08	−0.10	−0.02	−0.03	−0.09	0.18†	0.06	0.05	−0.07	0.02	−0.10	0.20*	0.08	0.36[a,*]	0.24
Curvature [Convex]	−0.23	0.22	−0.08	0.07	0.16	0.15	0.03	0.02	−0.10	0.09	0.02	0.01	0.02	0.01	0.13	0.12
Curvature [Concave]	−0.15	0.07	−0.28	0.20	−0.07	−0.01	0.05	−0.03	−0.03	−0.05	−0.04	−0.04	−0.29[a,*]	0.21	0.08	0.00
Plan [Convex]	−0.26[b,*]	0.24[b]	−0.16	0.14	−0.02	0.00	−0.08	0.06	−0.02	0.00	−0.03	0.01	0.03	0.01	−0.01	−0.01
Plan [Concave]	−0.17	0.08	−0.08	−0.01	−0.10	0.01	−0.06	−0.03	−0.05	−0.04	−0.12	0.03	−0.22[a,*]	0.13	−0.01	−0.08
Profile [Convex]	0.21	0.20	−0.28	0.27	−0.15	0.14	0.06	0.05	0.02	0.01	0.09	0.08	−0.07	0.06	−0.04	0.03
Profile [Concave]	0.00	−0.08	0.10	0.02	0.29	0.21	−0.04	−0.04	0.01	−0.07	−0.01	−0.07	0.20[a,*]	0.12	0.09	0.01
10 m																
Slope	−0.38*	−0.15	−0.45*	−0.08	−0.45*	−0.08	−0.45*	−0.08	−0.48*	−0.05	−0.65[a,*]	0.12	−0.35*	−0.18	−0.54*	0.01
Elevation	0.04	−0.08	0.08	−0.04	0.15	0.03	0.20†	0.08	0.16†	0.04	−0.06	−0.06	0.08	−0.04	0.45[a,*]	0.33
Curvature [Convex]	−0.33	0.18	0.24	0.09	−0.08	−0.07	−0.16	0.01	−0.12	−0.03	−0.23[a,*]	0.08	−0.08	−0.07	−0.15†	0.00
Curvature [Concave]	−0.15	0.09	0.24	0.18	0.29	0.23	0.14	0.08	−0.02	−0.04	0.01	−0.05	0.01	−0.05	0.15[a,†]	0.09
Plan [Convex]	−0.59[b,*]	0.47[b]	−0.02	−0.10	−0.18	0.06	−0.17	0.05	0.02	−0.10	−0.09	−0.03	−0.13	0.01	−0.08	−0.04
Plan [Concave]	−0.24	0.24	−0.36	0.36	0.17	0.17	−0.06	0.06	0.10	0.10	−0.09	0.09	0.04	0.04	0.13	0.13
Profile [Convex]	0.24	0.09	0.17	0.02	−0.06	−0.09	0.30[a,*]	0.15	0.10	−0.05	0.22*	0.07	−0.02	−0.13	0.21*	0.06
Profile [Concave]	0.22	0.15	−0.09	0.02	−0.07	0.00	−0.09	0.02	0.03	−0.04	−0.15†	0.08	−0.07	0.00	0.04	−0.03
20 m																
Slope	−0.41*	−0.15	−0.01	−0.55	−0.05	−0.51	−0.35*	−0.21	−0.56*	0.00	−0.70[a,*]	0.14	−0.31*	−0.25	−0.56*	0.00
Elevation	−0.14	0.02	0.01	−0.11	0.27†	0.15	0.28*	0.16	0.20*	0.08	−0.12†	0.00	0.06	−0.06	0.49[a,*]	0.37
Curvature [Convex]	0.11	−0.14	−0.24	−0.01	−0.44[b]	0.19[b,*]	−0.01	−0.24	−0.38[a,*]	0.13	−0.20*	−0.05	−0.11	−0.14	−0.34*	0.09
Curvature [Concave]	0.13	−0.01	−0.43	0.29	0.00	−0.14	0.19	0.05	0.12	−0.02	0.15†	0.01	0.20[a,†]	0.06	0.10	−0.04
Plan [Convex]	0.07	−0.15	−0.34	0.12	−0.23	0.01	−0.15	−0.07	−0.52[a,*]	0.30	−0.23*	0.01	−0.21†	−0.01	−0.13	−0.09
Plan [Concave]	0.32	0.24	−0.38	0.30	0.05	−0.03	0.02	−0.06	0.02	−0.06	0.11	0.03	0.10	0.02	0.13	0.05
Profile [Convex]	−0.32	0.05	0.11	−0.16	0.28	0.01	0.17	−0.10	0.33[a,*]	0.06	0.29*	0.02	0.21†	−0.06	0.24*	−0.03
Profile [Concave]	−0.50[b,*]	0.34[b]	0.21	0.05	0.00	−0.16	0.14	−0.02	−0.10	−0.06	−0.19[a,*]	0.03	−0.04	−0.12	−0.11	−0.05

A positive value of Δr_s indicates that the associated r_s increased with aspect stratification, where as a negative value of Δr_s indicates a decrease in associated r_s. $\Delta r_s = |r_{s2}| - |r_{s1}|$ where r_{s1} refers to the collective data (in Table 2) and r_{s2} to individual topographic variable data for a specific class aspect.

[a] The strongest r_s increase for each significant topographic variable under the same cell size with their Δr_s.

[b] Significant correlations that were not included in the interpretation because of lower *n*.

* $P < 0.01$.

† $P < 0.05$.

The correlation with elevation in the W aspect class was potentially improved with regard to the collective data set ($r_s = 0.49$, $P < 0.001$, and $\Delta r_s = 0.37$) at the 20-m resolution, suggesting that organic layer accumulation was more pronounced at higher, rather than at lower elevations (Figure 5B). An important increase in the correlation coefficient was also found in the W aspect class at the 1-, 5-, and 10-m resolutions with Δr_s values of 0.09, 0.24, and 0.33, respectively.

For all curvature variables (mean, plan, and profile), the correlation coefficient was generally higher than that for the collective data set, primarily at the 20-m resolution (Table 4). A significant increase in the correlation coefficient of convex-mean curvature ($r_s = -0.38$, $P < 0.01$, and $\Delta r_s = 0.13$) and convex-plan curvature ($r_s = -0.52$, $P < 0.01$, and $\Delta r_s = 0.30$) was found in the SE aspect class (Table 4) compared with that in the collective data set. These negative correlations suggest that shallow organic layers were, in large part, confined to convex areas (Figure 5C). Correlations for some plan curvature and profile curvature variables were substantially improved in the N aspect class (Table 4), but these were not included in the interpretation because of the lower sample size. For example, the correlation of the OLT and the north-facing concave-profile curvature had $r_s = -0.50$, $P < 0.01$, $\Delta r_s = 0.34$, and $n = 28$ (second column and last row of N aspect class in Table 4).

Regression Tree-Based Landscape Segmentation

In this study, the landscape was segmented with the 20-m resolution data because this scale showed a distinct advantage over the other DTMs (1, 5, and 10 m) in explaining accumulation and distribution of the organic layer across the landscape (Table 4). The landscape segmentation is illustrated in Figure 6 and in Table 5. At the landscape scale, regression tree analysis resulted in six landscape units with the topographic variables slope, aspect, and mean curvature classes, which were highly correlated with OLT ($P < 0.05$) (Figure 6A). Slope represented the best descriptor of the variability within OLT. The landscape was initially subdivided into two units with slope <2.3% and slope >2.3% (Figure 6A). Under slope conditions >2.3%, aspect was an important variable, but, in contrast, mean curvature was a more important variable for areas with slope ≤2.3%. Regression tree analysis showed higher OLT in areas with slopes ≤2.3% (landscape units A, B, and C) and lower OLT in areas with slopes >2.3% (landscape units D, E, and F, with mean depths of 29, 43, and 27 cm, respectively) (Table 5; Figure 6B). CVs

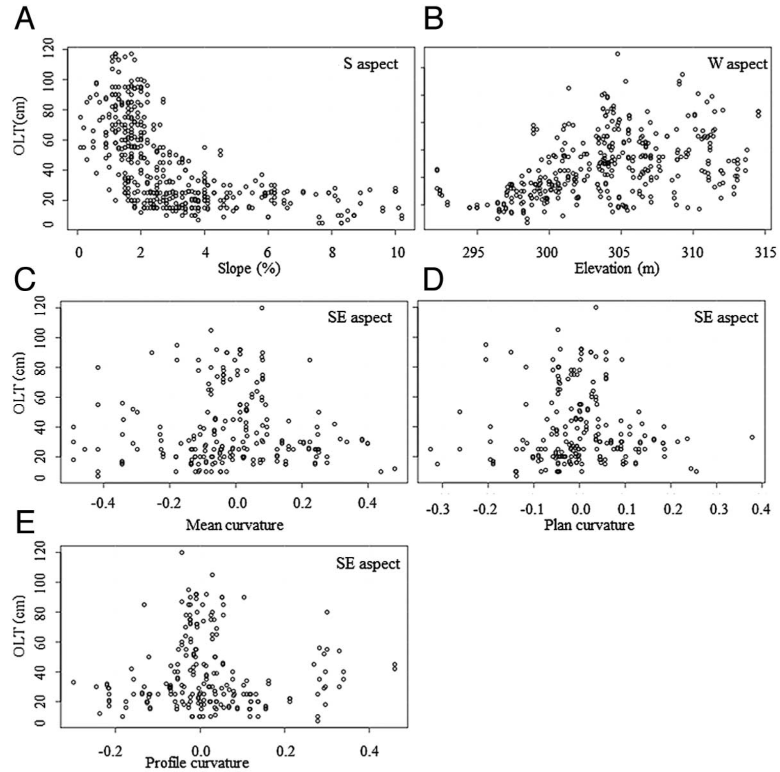

Figure 5. Relationships between selected topographic variables and OLT for areas with different aspects at 20-m resolution. (A) Slope. (B) Elevation. (C) Mean curvature. (D) Plan curvature. (E) Profile curvature.

for each group (Table 5) were lower than that for the collective data set (CV = 0.56), demonstrating that the landscape segmentation process markedly reduced the range of variability within each of the six landscape units.

Areas with Slope ≤2.3%

Areas with slopes ≤2.3% were further subdivided on the basis of slope (≤1.8% and >1.8%) and mean curvature (concave and convex), resulting in three landscape units (A, B, and C, with mean OLTs of 62, 56, and 48 cm, respectively). Field observations indicated that the deposit material type underlying each of the landscape units A, B, and C was composed of clay (86, 89, and 68%, respectively), till (13, 10, and 29%, respectively), and bedrock (1, 2, and 4%, respectively).

Areas with Slope >2.3%

Under conditions for which slopes were >2.3%, the data were most effectively split on the basis of slope (≤3.2% and >3.2%) and aspect class (N to S versus SW to NW) into three landscape units (D, E, and F). Regression tree analysis indicated that under slope conditions ≤3.2%, OLT was lower in southwest- to northwest-facing areas (landscape unit D) compared with those having north- to south-facing slopes (landscape unit E). Landscape units D and F had the lowest OLT of any units (Table 5). For landscape unit F, the nine highest values of OLT (up to 78 cm) are indicated as outliers in Figure 6B. Quantitative evidence from the field observations indicated that these values occurred where higher organic accumulations were observed on sloping terrain and were found in local depressions in the underlying bedrock. Indeed, landscape unit F had the second highest number of sampling points lying on bedrock (15% after landscape unit D with 57%).

Discussion

Relationships Between OLT and Topographic Variables at Different DTM Resolutions

Except for elevation, for which the correlation was consistently weak ($r_s = 0.12$) across all resolutions, correlation strength of topographic variables increased with decreasing resolution. In other words, lowering resolution caused details (i.e., shorter slopes) to be lost as resolution decreased and consequently tightened the variability range within the topographic variables studied. Of the four resolutions that were examined, the 20-m LiDAR-derived DTM showed the strongest correlations between topographic variables and OLT. This can be mainly attributed to topographic smoothing at the landscape scale that results from decreased resolution of DTMs. This finding was consistent with other studies that have found that small-scale topographic variation was lost with the use of a coarser digital elevation model (Potter et al. 1999, Grant 2004, Seibert et al. 2007, Wu et al. 2008).

Poor correlation between elevation and OLT indicated that elevation is a minor influence on OLT. When the collective data were used, elevation could not be used to discriminate between areas of higher and lower organic thicknesses over the entire study area. However, stratification of the data based on aspect classes revealed that elevation was positively correlated with OLT for areas having a west-facing slope, which was consistent with other studies, in which higher rates of paludification were found on plateaus (Gorozhankina 1997, Lavoie et al. 2005).

Not surprisingly, among all of the topographic variables that were studied, slope was the most important single control on OLT within the study area. Despite the observation of some strong relationships for some aspect classes (i.e., areas on south- and southeast-facing slopes), no major improvement in the strength of correlation

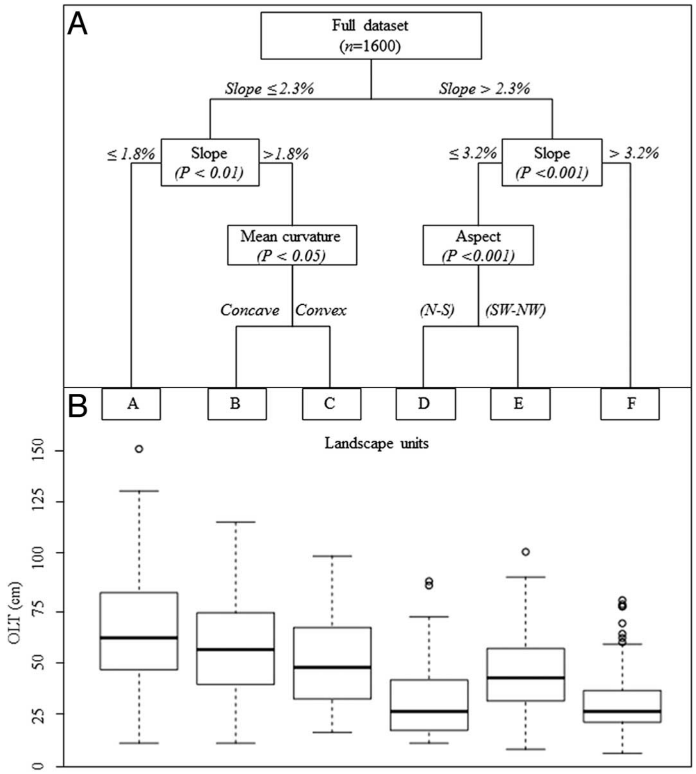

Figure 6. (A) Regression tree hierarchical landscape unit segmentation based on 20-m DTM. Each box corresponds to a final landscape unit (A−F), with the topographic variable on which the unit was subdivided listed and the range (value or identifier) for the topographic variable by which the unit was defined listed above. (B) Box plots of the OLT variability within each final landscape unit. A description of each component of the box and whiskers plot is given in Figure 3.

Table 5. Summary statistics for OLT by landscape unit for the study area.

Landscape units	n	Mean (cm)	SD (cm)	CV	Median (cm)
A	543	62	25	0.40	60
B	122	56	25	0.45	55
C	140	48	21	0.44	46
D	117	29	14	0.48	25
E	158	43	16	0.37	41
F	520	27	11	0.42	25

The landscape units correspond to those obtained by regression tree analysis and depicted in Figure 6. n represents number of sites.

coefficients was achieved with aspect stratification. Overall, it was apparent that the spatial distribution of OLT in our study area cannot be explained by simple bivariate relationships between OLT and individual topographic variables. In addition, the correlation analysis suggested a complex interrelationship between OLT and topographic variables, and, therefore, the use of a method that could split the study area into more homogeneous spatial units was justified.

Landscape Segmentation

Regression tree segmentation produced some landscape units with high variability that could be explained by local scale features. For example, depressions in the rock were locally observed on sloping terrain within landscape unit F. These topographic depressions, which were filled mostly with fibric and mesic materials, are scattered across the landscape and were probably created by episodic freeze-thaw events in the bedrock or by glacial erosion or may simply represent the surface roughness of the bedrock (Laamrani et al. 2013). This finding is consistent with earlier studies (Payette 2001, Simard et al. 2009), which found that paludification can occur on sloping well-drained terrain (up to 16%−20%) directly on bedrock where the humic material is almost inexistent and the fibric material is dominant (about 97%) (Larocque et al. 2003).

In addition to confirming the importance of slope effects on OLT at the landscape, which had been reported previously for the surface layers within the Clay Belt (i.e., Giroux et al. 2001, Simard et al. 2009), this study quantified the threshold (1.8%) at which slope could be used to discriminate units with the deepest organic layers (landscape unit A). Slope ≤1.8% could be used as a predictor for zones of soil saturation where a thick organic layer often accumulates. Furthermore, a slope threshold of 3.2% seemed to represent a cutpoint for discriminating between paludified and non-paludified areas. This study illustrated that even very small differences in slope, on the order of 1.4%, can significantly contribute to the estimation of paludified landscapes. This finding is consistent with those of previous researchers (Giroux et al. 2001, Simard et al. 2009, Lavoie et al. 2005), who calculated in the field differences in slope on the order of 0%−7% within the Clay Belt where slope is frequently less than 0.1% (Lavoie et al. 2007).

Contrary to our expectation, this study showed that overall, areas with slopes >2.3% and ≤3.2% exposed to the south and west (landscape unit E) were more prone to organic layer accumulation than those exposed to the north and east (landscape D). The higher OLT on west- and south-facing slopes may be tentatively explained by higher sphagnum moss growth stimulated by more radiation from the sun combined with higher moisture storage capacity. On the other hand, on areas with slopes exposed to the north and east (landscape unit D), dry soil conditions seems to prevail as a result of water movement causing a decrease in OLT. Seibert et al. (2007) found that the influence of aspect is largest at latitude 40−60°, which corresponds to the location of our investigated region.

Beside slope and aspect, mean curvature had the greatest influence on organic layer accumulation and contributed to the separation of units with varying OLT. Concave-mean curvature (landscape unit B) can be an indicator of areas of soil saturation, and organic layers often accumulate in lowlands. On the other hand, plan curvature and profile curvature variables were not selected by the regression tree analysis, and their effect was probably masked by the large number of almost flat areas on the landscape, because these two topographic variables represent flow dynamics across the surface (Table 1).

Despite various significant trends, the data exhibited obvious variability (expressed as data scattering). This kind of scattering is expected when one is working with a large data set that covers a range of different site conditions (Seibert et al. 2007). Another issue when one is working with large data sets is that even weak correlations are often statistically significant. In contrast, because of the large variability in site conditions, high correlation coefficients are not expected, and the correlations found may still have a physical meaning.

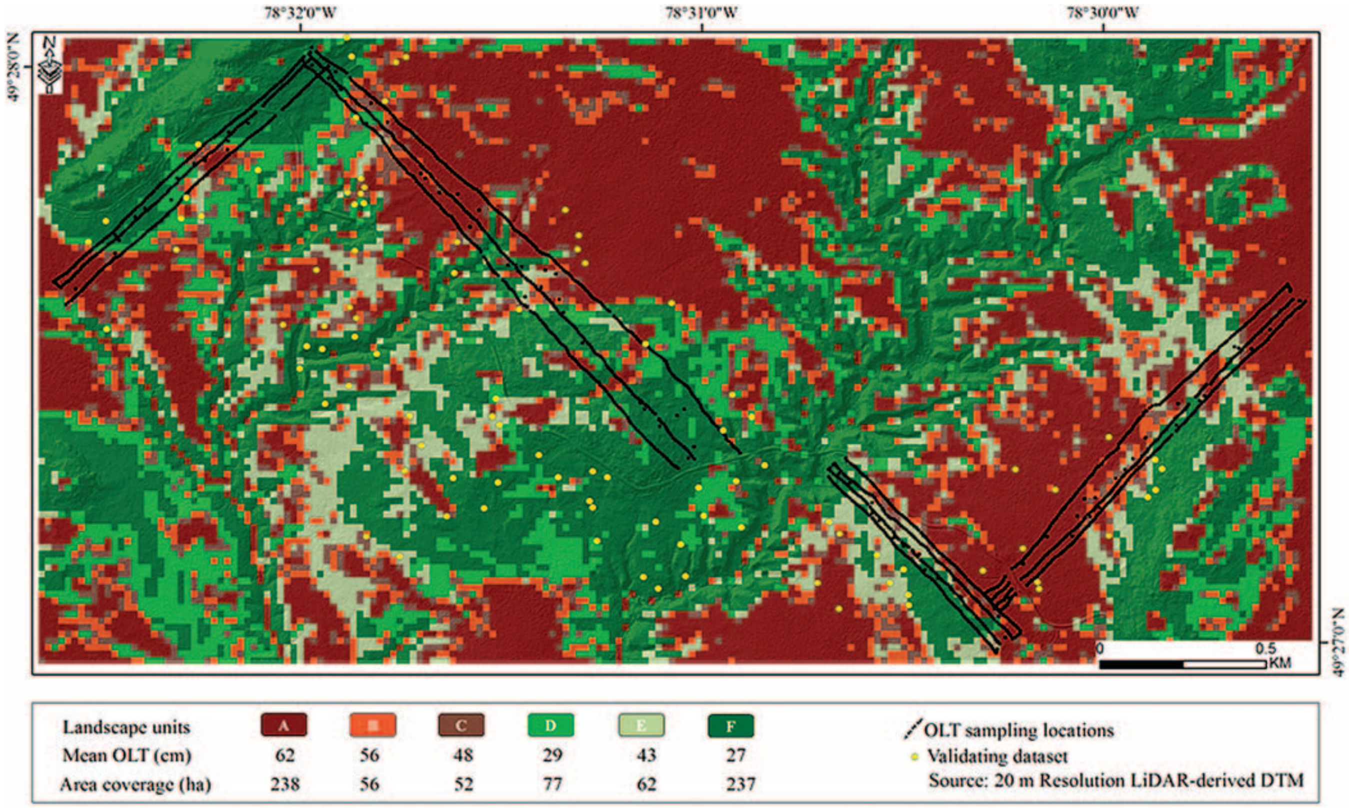

Figure 7. Thematic map showing the spatial distribution of the six resulting landscape units (A–F) across the study area. This map was produced using the regression tree rules based on the combination of slope, aspect, and mean curvature.

Management Implications and Future Research

The results of this study are important for landscape management for several reasons. (1) Understanding how surface topography is related to OLT is an important first step in predicting and mapping productivity across landscapes. This information will aid forest managers in predicting potential zones of saturation where organic layer often accumulates and will help them to adopt the appropriate forest management practices (i.e., field preparations, treatments, and replanting). For example, slope can be used to better manage forest resources where high soil moisture limits productivity. (2) To maintain or improve forest productivity in the Clay Belt region, management strategies should focus on sloping sites (i.e., >2.3%) rather than on almost flat sites (≤1.8%). The latter are associated with a deep organic layer that is often not suitable for tree plantations (Lafleur et al. 2010) and provide few ecological or economic motives to manage soils with low slopes (Simard et al. 2009). (3) We expect that the use of LiDAR-derived topographic variables as sources of information in environmental management will increase in the future, especially as the availability of precise digital data increases. The potential of LiDAR data to provide spatial detail for planning and the optimization of forest management activities in boreal forests has been demonstrated in a previous study (Woods et al. 2011). (4) This study is part of a larger project that deals with the effects of environmental variables and forest harvesting on paludification and was conducted before implementation of recent forest management. Therefore, results from this study could be used to determine the long-term impact of forest management practices (i.e., forest harvesting, field preparation treatments, and replanting) on the original organic layer proprieties.

Our segmentation of the landscape illustrated that areas with higher slopes were associated with thinner organic layers, as did that of Simard et al. (2009), who found that rates of organic layer accumulation at the plot scale were highest on flatter sites and diminished with increasing slope on the Clay Belt. This result supported our hypothesis that topography has a significant influence on the spatial distribution of OLT and that these relationships can be used for partitioning the landscape and, therefore, can help in future planning of landscape management.

The combination of topographic information (from remotely sensed LiDAR data) with field measurement has the potential to be useful for defining both promising and vulnerable areas for forest management. For instance, landscape units A and B seem to represent areas with conditions that may be less favorable for tree growth because the presence of a thick organic layer combined with wet conditions on flat terrain is expected to limit the use of equipment for mechanical site preparation and harvesting within the highly paludified areas (Lavoie et al. 2007). This was supported by ongoing studies that deal with the effect of OLT and slope on forest productivity (A. Laamrani and N. Fenton, Université du Québec en Abitibi-Témiscamingue, unpubl. observ., 2013), which found that on average, landscape units A and B showed the lowest stand volumes (estimated for trees with dbh >9 cm) with 104 and 125 m^3/ha, respectively. On the other hand, landscape units D and F with estimated stand volumes of 204 and 207 m^3/ha, respectively, seem to represent very attractive conditions for forest managers.

Once the regression trees were completed, they provided a set of decision rules that defined the range of conditions, i.e., values of the predictor variables, which are best used to predict each landscape unit. We used these rules to create a thematic map of the spatial distribution of the resulting landscape units across the study area (Figure 7). When forest inventory maps from the MRNQ were superimposed on the regression tree-derived thematic map using ArcGIS 10.0 (ESRI 2011), there was good statistical matching (71%; validating data set $n = 97$) (Figure 7) between the landscape unit distribution and forest management area status (suitable or not). Thus, regression tree and the derived thematic map might be useful for identifying and predicting spatial differences in terms of OLT on the landscape, which would be of interest to facilitate forest management in areas of limited data availability within the Clay Belt region. In addition, the regression tree breakdown of the data into the six landscape units was statistically and visually related to the distribution of three landscape topographic variables (slope aspect and mean curvature; maps of each of these variables are not shown in this study).

Finally, our study illustrated not only the potential of some topography variables to explain the occurrence of highly paludified areas but also the need for further studies. Our future work will focus on the importance of mineral soil topography on the spatial distribution of the organic layer over the same landscape, especially if topographic variables could be used to discriminate between the two common types of paludification (successional and edaphic) (for an overview of paludification types, see Fenton et al. 2009).

Conclusions

This study demonstrated that the relationship between OLT and most individual topographic variables (obtained from LiDAR-derived DTMs) is consistently weak. Slope was found to have a significant role in the spatial distribution of OLT at the landscape scale. A regression tree analysis partitioned landscape data into six statistically different landscape units. Further, the mean OLT of each landscape unit was either significantly different from that of all other units or the lack of differences could be explained by meaningful field observations. Landscape segmentation served to discriminate between areas of greater and lesser OLT based on slope, aspect, and mean curvature variables. Indeed, higher OLT was confined to gentle sloping areas ($\leq$1.8%). For areas with relatively higher slopes ($>$2.3% and $\leq$3.2%), organic layers were also found to be deeper for south-facing slopes than north-facing slopes. A thematic productive map of the distribution of the resulting six landscape unit was generated using the regression tree based on the combination of slope, aspect, and mean curvature. This thematic map was useful for recognizing both vulnerable and promising areas (overall matching of 71%) for forest management. To summarize, relationships between OLT and topographic variables at the landscape scale confirmed the importance of topography on OLT, which was previously noted at the plot scale within the Clay Belt. Finally, the most accurate results were obtained from the 10- and 20-m resolution LiDAR-derived data rather than from that of higher resolution (1 and 5 m).

Literature Cited

CRAWFORD, R.M.M., C.E. JEFFREE, AND W.G. REES. 2003. Paludification and forest retreat in northern oceanic environments. *Ann. Bot. (Lond.)* 91(Spec. Iss. Jan.):213–226.

DE'ATH, G., AND K.E. FABRICIUS. 2000. Classification and regression trees: A powerful yet simple technique for ecological data analysis. *Ecology* 81(11):3178–3192.

EMILI, L.A., J.S. PRICE, AND D.F. FITZGERALD. 2006. Hydrogeological influences on forest community type along forest-peatland complexes in coastal British Columbia. *Can. J. For. Res.* 36(8):2024–2037.

ENVIRONMENTAL SYSTEMS RESEARCH INSTITUTE. 2011. *ArcGIS Desktop: Release 10. Environmental Systems Research Institute, Redlands, CA, USA.* Available online at help.arcgis.com/en/arcgisdesktop/10.0/help/; last accessed Nov. 23, 2013.

ENVIRONMENT CANADA. 2011. *Canadian climate normals, 1971–2000.* Available online at www.climate.weatheroffice.gc.ca/climate_normal; last accessed Nov. 23, 2013.

FENTON, N., N. LECOMTE, S. LÉGARÉ, AND Y. BERGERON. 2005. Paludification in black spruce (*Picea mariana*) forests of eastern Canada: Potential factors and management implications. *For. Ecol. Manage.* 213(1–3):151–159.

FENTON, N.J., AND Y. BERGERON. 2007. Sphagnum community change after partial harvest in black spruce boreal forests. *For. Ecol. Manage.* 242(1):24–33.

FENTON, N.J., M. SIMARD, AND Y. BERGERON. 2009. Emulating natural disturbances: The role of silviculture in creating even-aged and complex structures in the black spruce boreal forest of eastern North America. *J. For. Res.* 14(5):258–267.

GIROUX, J.F., Y. BERGERON, AND J.J. VEILLETTE. 2001. Dynamics and morphology of giant circular patterns of low tree density in black spruce stands in northern Quebec. *Can. J. Bot.* 79(4):420–428.

GOROZHANKINA, S.M. 1997. Paludification in the Tsentral'no-Sibirskii biosphere reserve (the Yenisei region of Siberia). *Russ. J. Ecol.* 28(2):67–72.

GRANT, R.F. 2004. Modeling topographic effects on net ecosystem productivity of boreal black spruce forests. *Tree Physiol.* 24(1):1–18.

HÄRING, T., E. DIETZ, S. OSENSTETTER, T. KOSCHITZKI, AND B. SCHRÖDER. 2012. Spatial disaggregation of complex soil map units: A decision tree-based approach in Bavarian forest soils. *Geoderma* 185–186:37–47.

HODGSON, M.E., J. JENSEN, G. RABER, J. TULLIS, B.A. DAVIS, G. THOMPSON, AND K. SCHUCKMAN. 2005. An evaluation of lidar-derived elevation and terrain slope in leaf-off conditions. *Photogramm. Eng. Remote Sens.* 71(7):817–823.

HODGSON, M.E., J.R. JENSEN, L. SCHMIDT, S. SCHILL, AND B. DAVIS. 2003. An evaluation of LIDAR- and IFSAR-derived digital elevation models in leaf-on conditions with USGS level 1 and level 2 DEMs. *Remote Sens. Environ.* 84(2):295–308.

HOTHORN, T., K. HORNIK, AND A. ZEILEIS. 2006. Unbiased recursive partitioning: A conditional inference framework. *J. Comput. Graph. Stat.* 15(3):651–674.

HYDE, P., R. DUBAYAH, B. PETERSON, J.B. BLAIR, M. HOFTON, C. HUNSAKER, R. KNOX, AND W. WALKER. 2005. Mapping forest structure for wildlife habitat analysis using waveform lidar: Validation of montane ecosystems. *Remote Sens. Environ.* 96(3–4):427–437.

JOHNSON, K.D., F.N. SCATENA, A.H. JOHNSON, AND Y. PAN. 2009. Controls on soil organic matter content within a northern hardwood forest. *Geoderma* 148(3–4):346–356.

LAAMRANI, A., O. VALERIA, L.Z. CHENG, Y. BERGERON, AND C. CAMERLYNCK. 2013. The use of ground penetrating radar for remote sensing the organic layer-mineral soil interface in paludified boreal forests. *Can. J. Remote Sens.* 39(1):74–88.

LAFLEUR, B., N.J. FENTON, D. PARÉ, M. SIMARD, AND Y. BERGERON. 2010. Contrasting effects of season and method of harvest on soil properties and the growth of black spruce regeneration in the boreal forested peatlands of eastern Canada. *Silva Fenn.* 44(5):799–813.

LAROCQUE, I., Y. BERGERON, I.D. CAMPBELL, AND R.H.W. BRADSHAW. 2003. Fire-induced decrease in forest cover on a small rock outcrop in the Abitibi region of Québec, Canada. *Ecoscience* 10(4):515–524.

Lavoie, M., D. Paré, N. Fenton, A. Groot, and K. Taylor. 2005. Paludification and management of forested peatlands in Canada: A literature review. *Environ. Rev.* 13(2):21–50.

Lavoie, M., K. Harper, D. Paré, and Y. Bergeron. 2007. Spatial pattern in the organic layer and tree growth: A case study from regenerating *Picea mariana* stands prone to paludification. *J. Veg. Sci.* 18(2): 213–222.

Lecomte, N., M. Simard, Y. Bergeron, A. Larouche, H. Asnong, and P.J.H. Richard. 2005. Effects of fire severity and initial tree composition on understorey vegetation dynamics in a boreal landscape inferred from chronosequence and paleoecological data. *J. Veg. Sci.* 16(6):665–674.

Martin, W.K.E., and V.R. Timmer. 2006. Capturing spatial variability of soil and litter properties in a forest stand by landform segmentation procedures. *Geoderma* 132(1–2):169–181.

Mulder, V.L., S. de Bruin, M.E. Schaepman, and T.R. Mayr. 2011. The use of remote sensing in soil and terrain mapping—A review. *Geoderma* 162(1–2):1–19.

Payette, S. 2001. Les principaux types de tourbières. P. 39–89 in *Écologie des tourbières du Québec-Labrador: Une perspective nord-américaine*, Payette, S., and L. Rochefort (eds.). Presses de l'Université Laval, Laval, QC, Canada.

Pennock, D.J., and M.D. Corre. 2001. Development and application of landform segmentation procedures. *Soil Till. Res.* 58(3–4):151-162.

Potter, C.S., J.C. Coughlan, and V. Brooks. 1999. Investigations of BOREAS spatial data in support of regional ecosystem modeling. *J. Geophys. Res. Atmos.* 104(D22):27771–27788.

R Development Core Team. 2011. *R: A language and environment for statistical computing*. R Foundation for Statistical Computing, Vienna, Austria.

Rothwell, J.J., M.N. Futter, and N.B. Dise. 2008. A classification and regression tree model of controls on dissolved inorganic nitrogen leaching from European forests. *Environ. Pollut.* 156(2):544–552.

Seibert, J., J. Stendahl, and R. Sorensen. 2007. Topographical influences on soil properties in boreal forests. *Geoderma* 141(1–2):139–148.

Simard, M., P.Y. Bernier, Y. Bergeron, D. Paré, and L. Guérine. 2009. Paludification dynamics in the boreal forest of the James Bay Lowlands: Effect of time since fire and topography. *Can. J. For. Res.* 39(3):546–552.

Simard, M., N. Lecomte, Y. Bergeron, P.Y. Bernier, and D. Pare. 2007. Forest productivity decline caused by successional paludification of boreal soils. *Ecol. Appl.* 17(6):1619–1637.

Southee, F.M., P.M. Treitz, and N.A. Scott. 2012. Application of lidar terrain surfaces for soil moisture modeling. *Photogramm. Eng. Remote Sens.* 78(12):1241–1251.

Veillette, J.J. 1994. Evolution and paleohydrology of glacial Lakes Barlow and Ojibway. *Q. Sci. Rev.* 13(9–10):945–971.

Vygodskaya, N.N., P.Y. Groisman, N.M. Tchebakova, J.A. Kurbatova, O. Panfyorov, E.I. Parfenova, and A.F. Sogachev. 2007. Ecosystems and climate interactions in the boreal zone of northern Eurasia. *Environ. Res. Lett.* 2(4).

Webster, K.L., I.F. Creed, F.D. Beall, and R.A. Bourbonnière. 2011. A topographic template for estimating soil carbon pools in forested catchments. *Geoderma* 160(3–4):457–467.

Woods, M., D. Pitt, M. Penner, K. Lim, D. Nesbitt, D. Etheridge, and P. Treitz. 2011. Operational implementation of a LiDAR inventory in boreal Ontario. *For. Chron.* 87(4):512–528.

Work, T.T., B. St-Onge, and J.M. Jacobs. 2011. Response of female beetles to LIDAR derived topographic variables in Eastern boreal mixedwood forests (Coleoptera, Carabidae). *ZooKeys* 147:623–639.

Wu, W., Y. Fan, Z. Wang, and H. Liu. 2008. Assessing effects of digital elevation model resolutions on soil-landscape correlations in a hilly area. *Agr. Ecosyst. Environ.* 126(3–4):209–216.